

# Theoretical Studies of Inorganic and Organometallic Reaction Mechanisms. 14. $\beta$ -Hydrogen Transfer and Alkene/Alkyne Insertion at a Cationic Iridium Center

Shuqiang Niu, Snežana Zarić,<sup>†</sup> Craig A. Bayse, Douglas L. Strout,<sup>‡</sup> and Michael B. Hall\*

Department of Chemistry, Texas A&M University, College Station, Texas 77843

Received May 26, 1998

Recent experimental work shows that alkanes can be activated by  $\text{Cp}^*\text{Ir}(\text{PMe}_3)(\text{CH}_3)^+$  at room temperature to generate olefin complexes. The reaction begins with alkane activation by oxidative addition (OA) followed by reductive elimination (RE) of methane and then olefin formation by the  $\beta$ -H transfer from the bound alkyl. Ab initio calculations and density functional theory (DFT) studies of ethane activation by  $\text{CpIr}(\text{PH}_3)(\text{CH}_3)^+$  (**1**) to generate  $\text{CpIr}(\text{PH}_3)(\eta^2\text{-C}_2\text{H}_4)(\text{H})^+$  (**7**) show that the  $\beta$ -H transfer from  $\text{CpIr}(\text{PH}_3)(\text{C}_2\text{H}_5)^+$  (**5**) to **7** is exothermic by 12 and 16 kcal/mol with a very low barrier of 0.7 and 0.4 kcal/mol at the DFT and CCSD levels, respectively. Thus, the rate-determining step in alkane dehydrogenation to olefin complexes by  $\text{Cp}^*\text{Ir}(\text{PMe}_3)(\text{CH}_3)^+$  is the alkane OA step. These results are in very good agreement with the experimental work of Bergman and co-workers. A strong stabilizing interaction between either ethylene or acetylene and  $\text{CpIr}(\text{PH}_3)(\text{CH}_3)^+$  leads to high activation barriers (25–36 kcal/mol) for the insertion processes of ethylene or acetylene. In comparison to ethylene, the insertion reaction of acetylene with the  $\text{CpIr}(\text{PH}_3)(\text{CH}_3)^+$  complex is more favorable. Thus, the dimerization of terminal alkynes catalyzed by cationic iridium complexes is plausible.

## Introduction

Oxidative addition, reductive elimination, migratory insertion,  $\beta$ -hydrogen transfer,  $\sigma$ -bond metathesis, and nucleophilic addition reactions are fundamental steps of importance in transition-metal-catalyzed processes.<sup>1</sup> Numerous experimental and theoretical studies have been undertaken in order to understand these fundamental transformations.<sup>1,2</sup> Recent progress in computational chemistry has shown that many important chemical and physical properties of the species involved in these reactions can be predicted from first principles by various efficient computational techniques. This ability is especially important in those cases where experimental results are difficult to obtain.<sup>1–3</sup>

In early work, Crabtree and co-workers described an Ir(III) system,  $\text{Ir}(\text{H})_2(\text{Me}_2\text{CO})(\text{PPh}_3)_2^+$ , which thermally dehydrogenates cyclopentenes to cyclopentadienyl complexes.<sup>4</sup> Recently, Bergman and co-workers reported

another Ir(III) system,  $\text{Cp}^*\text{Ir}(\text{PMe}_3)(\text{CH}_3)^+$  ( $\text{Cp}^* = \eta^5\text{-C}_5(\text{CH}_3)_5$ ), which thermally activates alkanes in the solution phase at unprecedentedly low temperatures to generate olefin complexes.<sup>5</sup> Most recently, Xu et al. have described an iridium(III) catalytic system,  $(\text{PCP})\text{-Ir}(\text{H})_2$  ( $\text{PCP} = \eta^3\text{-C}_6\text{H}_3(\text{PBU}^t)_2\text{-1,3}$ ), which catalyzes the dehydrogenation of alkanes to the corresponding alkenes and dihydrogen.<sup>6</sup> Common features of these reactions are oxidative addition/reductive elimination (OA/RE) and then  $\beta$ -H transfer to form  $[\text{Ir}](\text{H})(\eta^2\text{-C}_2\text{H}_4)^+$  as an intermediate or product. Recently, several experimental and theoretical studies have been performed to elucidate details on the OA/RE stages of these reactions.<sup>7,8</sup>

Since early metals are especially good at polymerizing olefins (Ziegler–Natta catalysts being the archetype)

<sup>†</sup> Permanent address: Faculty of Chemistry, University of Belgrade, Studentski trg 16, 11001 Beograd, Yugoslavia.

<sup>‡</sup> New address: Environmental Molecular Sciences Laboratory, Pacific Northwest National Laboratory, Richland, WA 99352.

(1) (a) Elschenbroich, C.; Salzer, A. *Organometallics*; VCH: New York, 1989. (b) Crabtree, R. H. *The Organometallic Chemistry of the Transition Metals*; Wiley: New York, 1988. (c) Parshall, G. W. *Homogeneous Catalysis*; Wiley: New York, 1980.

(2) (a) Koga, K.; Morokuma, K. *Chem. Rev.* **1991**, *91*, 823. (b) Musaev, D. G.; Morokuma, K. In *Advances in Chemical Physics*; Prigogine, I., Rice, S. A., Eds.; Wiley: New York, 1996; Vol. XCV, p 61. (c) Siegbahn, P. E. M.; Blomberg, M. R. A. In *Theoretical Aspects of Homogeneous Catalysis. Applications of Ab Initio Molecular Orbital Theory*; van Leeuwen, P. W. N. M., van Lenthe, J. H., Morokuma, K., Eds.; Kluwer: Hingham, MA, 1995.

(3) *Reviews in Computational Chemistry*; Lipkowitz, K. B., Boyd, D. B., Eds.; VCH: New York, 1990–1996; Vols. 1–7.

(4) (a) Crabtree, R. H.; Mihelcic, J. M.; Quirk, J. M. *J. Am. Chem. Soc.* **1979**, *101*, 7738. (b) Baudry, M. J.; Ephritikine, M.; Felkin, H.; Holmes-Smith, R. *J. Chem. Soc., Chem. Commun.* **1983**, 788. (c) Baudry, M. J.; Crabtree, R. H.; Parnell, C. P.; Uriarte, R. *J. Organometallics* **1984**, *3*, 816.

(5) (a) Arndtsen, B. A.; Bergman, R. G. *Science* **1995**, *270*, 1970. (b) Burger, P.; Bergman, R. G. *J. Am. Chem. Soc.* **1993**, *115*, 10462. (c) For a review see: Lohrenz, J. C. W.; Jacobsen, H. *Angew. Chem., Int. Ed. Engl.* **1996**, *35*, 1305.

(6) (a) Xu, W.-W.; Rosini, G. P.; Gupta, M.; Jensen, C. M.; Kaska, W. C.; Krogh-Jespersen, K.; Goldman, A. S. *Chem. Commun.* **1997**, 2273. (b) Roubi, M. *Chem. Eng. News* **1997**, 75(49), 25.

(7) (a) Strout, D.; Zarić, S.; Niu, S.-Q.; Hall, M. B. *J. Am. Chem. Soc.* **1996**, *118*, 6068. (b) Su, M.-D.; Chu, S.-Y. *J. Am. Chem. Soc.* **1997**, *119*, 5373. (c) Niu, S.-Q.; Strout, D.; Zarić, S.; Bayse, C. A.; Hall, M. B. *ACS Symp. Ser.*, in press. (d) Niu, S.-Q.; Hall, M. B. *J. Am. Chem. Soc.* **1998**, *120*, 6169. (e) Niu, S.-Q.; Hall, M. B. *J. Am. Chem. Soc.*, in press.

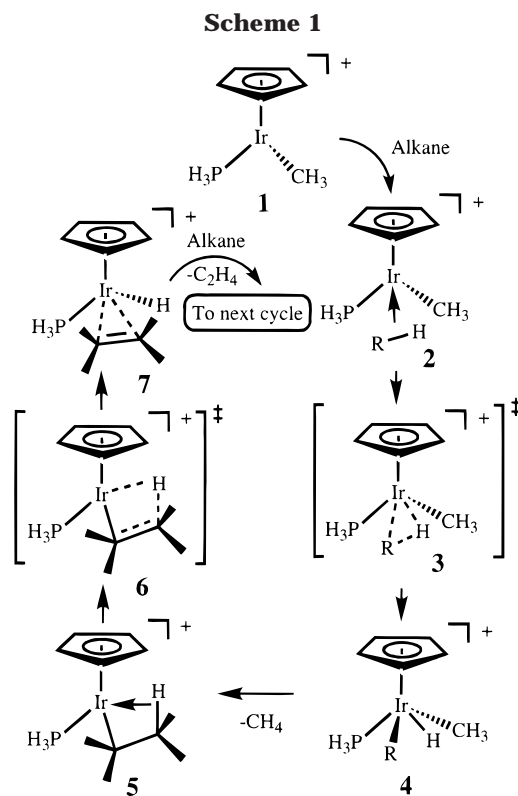
(8) (a) Hinderling, C.; Plattner, D. A.; Chen, P. *Angew. Chem., Int. Ed. Engl.* **1997**, *36*, 243. (b) Hinderling, C.; Feichtings, D.; Plattner, D. A.; Chen, P. *J. Am. Chem. Soc.* **1997**, *119*, 10793. (c) Luecke, H. F.; Bergman, R. G. *J. Am. Chem. Soc.*, **1997**, *119*, 11538.

and oligomerizing alkynes,<sup>1,9</sup> the higher oxidation state Ir(III) system, if it has some early-transition-metal character, could catalyze other reactions typical of early-metal systems such as polymerization. Although these Ir(III) systems have not been studied experimentally as polymerization or oligomerization catalysts, there are a series of Fe(II), Co(III), Ni(II), Pd(II), and Ru(II) complexes which have been shown to catalyze these reactions.<sup>10</sup> In this work, the  $\beta$ -hydrogen transfer of Ir(III) ethyl and vinyl complexes and the ethylene and acetylene insertion into the Ir(III)–CH<sub>3</sub>  $\sigma$ -bond are investigated with density functional theory (DFT) and ab initio molecular orbital theory.

### Computational Details

The geometry optimizations in this work have been performed using DFT<sup>11</sup> methods, specifically the Becke three-parameter hybrid exchange functional<sup>11b-d</sup> and the Lee–Yang–Parr correlation functional<sup>11e</sup> (B3LYP). The transition states were optimized using a quasi-Newton method and characterized by determining the number of imaginary frequencies.<sup>12</sup> For a direct estimation of electron correlation effects and accurate reaction energetics, coupled cluster with singles and doubles (CCSD)<sup>13</sup> calculations were carried out on the DFT-optimized geometry. To simplify the calculations, we replaced the phosphine group and Cp\* ring in the actual molecules by PH<sub>3</sub> and a Cp ring (Cp =  $\eta^5$ -C<sub>5</sub>H<sub>5</sub>).<sup>14</sup> Differences in the zero-point energy (ZPE) and thermal corrections to the reaction energy tend to be small. For example, we determined ZPE and thermal corrections for the transformations H<sub>2</sub>Ti(CHCH<sub>2</sub>)(H) → H<sub>2</sub>Ti( $\eta^2$ -CH<sub>2</sub>CH<sub>2</sub>) and H<sub>2</sub>Ti( $\eta^2$ -CH<sub>2</sub>CH<sub>2</sub>)(H)<sup>+</sup> → H<sub>2</sub>TiCH<sub>2</sub>CH<sub>3</sub><sup>+</sup> and found the ZPE correction to be 2.6 and 2.5 kcal/mol and thermal correction to be 2.0 and 1.4 kcal/mol, respectively.<sup>15</sup>

Iridium is described by a modified version of the Hay and Wadt basis set with effective core potentials<sup>16a</sup> (ECP). The modifications to the double- $\zeta$  basis set were made by Couty and Hall<sup>16b</sup> and give a better representation of the 6p space. The result is a [3s3p2d] contracted basis set for iridium, where the 5s and 5p basis functions are left totally contracted but 6s, 6p, and 5d are split (41), (41), and (41), respectively. The carbons and hydrogens are described using the Dunning–Huzinaga double- $\zeta$  basis functions.<sup>17a</sup> The Hay and Wadt ECP



double- $\zeta$  basis set was used for phosphorus.<sup>17b</sup> The outermost p-functions have been shown to be important valence functions for transition metals.<sup>16b</sup> Thus, this basis set does not have any polarization functions. In previous work,<sup>7d</sup> we have shown that the addition of polarization functions on the ligand atoms are important, especially for metal–ligand binding energies, where addition of polarization functions decreases the C–H bond activation barrier and decreases the OA reaction's endothermicity by about 4 and 3 kcal/mol, respectively. At the B3LYP and CCSD//B3LYP levels, the association energies of methane, ethylene, and acetylene with the CpIr(PH<sub>3</sub>)(CH<sub>3</sub>)<sup>+</sup> complex have been corrected for the basis-set superposition error (BSSE).<sup>17c</sup>

All ab initio and DFT calculations were performed with GAMESS-UK<sup>18</sup> and GAUSSIAN94 programs<sup>19</sup> at the Cornell Theory Center on an IBM ES6000 and a Scalable Power-parallel (SP2), at Cray Research, Inc. on the Cray C90, at the Supercomputer Center of Texas A&M University and the Department of Chemistry on Silicon Graphics Power Challenge servers, and on Silicon Graphics Power Indigo II IMPACT 10000 workstations in our laboratory and at the Institute of Scientific Computation (ISC) of Texas A&M University.

### Results and Discussion

**Alkane Dehydrogenation by Cp\*Ir(PH<sub>3</sub>)(CH<sub>3</sub>)<sup>+</sup> (1).** The experimental work of Bergman and co-workers shows that alkanes can be activated by Cp\*Ir(PMe<sub>3</sub>)(CH<sub>3</sub>)<sup>+</sup> at room temperature to generate olefin com-

(9) (a) Boor, J., Jr. *Ziegler–Natta Catalysts and Polymerization*; Academic Press: New York, 1979. (b) Allen, G. B. *Comprehensive Polymer Science*; Pergamon Press: Oxford, U.K., 1989.

(10) (a) Crackness, R. B.; Orpen, A. G.; Spencer, J. L. *J. Chem. Soc., Chem. Commun.* **1984**, 326. (b) Brookhart, M.; Schmidt, G. F.; Lincoln, D.; Rivers, D. S. *Transition Metal Catalyzed Polymerizations*; Quirk, R., Ed.; Cambridge University Press: Cambridge, U.K., 1988. (c) Schmidt, G. F.; Brookhart, M. *J. Am. Chem. Soc.* **1985**, *107*, 1443. (d) Trost, B. M.; Sorum, M. T.; Chan, C.; Harms, A. E.; Rühter, G. *J. Am. Chem. Soc.* **1997**, *119*, 698. (e) Slugovc, C.; Mereiter, K.; Zobetz, E.; Schmid, R.; Kirchner, K. *Organometallics* **1996**, *15*, 5275. (f) Freemantle, M. *Chem. Eng. News* **1998**, *76*(15), 12.

(11) (a) Parr, R. G.; Yang, W. *Density-Functional Theory of Atoms and Molecules*; Oxford University Press: Oxford, U.K., 1989. (b) Becke, A. D. *Phys. Rev.* **1988**, *A38*, 3098. (c) Becke, A. D. *J. Chem. Phys.* **1993**, *98*, 1372. (d) Becke, A. D. *J. Chem. Phys.* **1993**, *98*, 5648. (e) Lee, C.; Yang, W.; Parr, R. G. *Phys. Rev.* **1988**, *B37*, 785.

(12) Schlegel, H. B. *Theor. Chim. Acta* **1984**, *66*, 33.

(13) (a) Bartlett, R. J. *Annu. Rev. Phys. Chem.* **1981**, *32*, 359. (b) Scuseria, G. E.; Schaefer, H. F., III. *J. Chem. Phys.* **1989**, *90*, 3700.

(14) (a) Song, J.; Hall, M. B. *J. Am. Chem. Soc.* **1993**, *115*, 327. (b) Sulfab, Y.; Basolo, F.; Rheingold, A. L. *Organometallics* **1989**, *8*, 2139.

(15) Jiménez-Cataño, R.; Niu, S.-Q.; Hall, M. B. *Organometallics* **1997**, *16*, 1962.

(16) (a) Hay, P. J.; Wadt, W. R. *J. Chem. Phys.* **1985**, *82*, 299. (b) Couty, M.; Hall, M. B. *J. Comput. Chem.* **1996**, *17*, 1359.

(17) (a) Dunning, T. H., Jr.; Hay, P. J. In *Modern Theoretical Chemistry*; Schaefer, H. F., III., Ed.; Plenum: New York, 1976. (b) Wadt, W. R.; Hay, P. J. *J. Chem. Phys.* **1985**, *82*, 284. (c) The BSSE corrections for the reaction systems were performed using model systems: (H)Ir(PH<sub>3</sub>)(H)(L)<sup>+</sup> (L = CH<sub>4</sub>, C<sub>2</sub>H<sub>2</sub>, C<sub>2</sub>H<sub>4</sub>).

(18) Guest, M. F.; Kendrick, J.; van Lenthe, J. H.; Schoeffel, K.; Sherwood, P. GAMESS-UK; Daresbury Laboratory: Warrington, WA4 4AD, U.K., 1994.

(19) Frisch, M. J.; Trucks, G. W.; Schlegel, H. B.; Gill, P. M. W.; Johnson, B. G.; Robb, M. A.; Cheeseman, J. R.; Keith, T. A.; Petersson, G. A.; Montgomery, J. A.; Raghavachari, K.; Al-Laham, M. A.; Zakrzewski, V. G.; Ortiz, J. V.; Foresman, J. B.; Cioslowski, J.; Stefanov, B. B.; Nanayakkara, A.; Challacombe, M.; Peng, C. Y.; Ayala, P. Y.; Chen, W.; Wong, M. W.; Andres, J. L.; Replogle, E. S.; Gomperts, R.; Martin, R. L.; Fox, D. J.; Binkley, J. S.; Defrees, D. J.; Baker, J.; Stewart, J. P.; Head-Gordon, M.; Gonzalez, C.; Pople, J. A. Gaussian 94 (Revision D.2); Gaussian, Inc., Pittsburgh, PA, 1995.

**Table 1.** Relative Energies ( $\Delta E$ , kcal/mol) of the Reactions (A)–(E) by B3LYP and CCSD//B3LYP

structure	$\Delta E$	
	B3LYP	CCSD//B3LYP
A. C–H Activation Reaction of Methane <sup>7c</sup>		
CpIr(PH <sub>3</sub> )(CH <sub>3</sub> ) <sup>+</sup> , CH <sub>4</sub> ( <b>1</b> + methane)	1.03 (–0.19) <sup>a</sup>	6.43 (0.90) <sup>a</sup>
CpIr(PH <sub>3</sub> )(CH <sub>3</sub> )(CH <sub>4</sub> ) <sup>+</sup> ( <b>2</b> )	0.00	0.00
CpIr(PH <sub>3</sub> )(CH <sub>3</sub> )(H)(CH <sub>3</sub> ) <sup>+</sup> ( <b>3</b> (TS <sub>2–4</sub> ))	11.54	9.97
CpIr(PH <sub>3</sub> )(CH <sub>3</sub> )(H)(CH <sub>3</sub> ) <sup>+</sup> ( <b>4</b> )	4.41	0.81
B. $\beta$ -H Transfer of CpIr(PH <sub>3</sub> )(C <sub>2</sub> H <sub>5</sub> ) <sup>+</sup>		
CpIr(PH <sub>3</sub> )(C <sub>2</sub> H <sub>5</sub> ) <sup>+</sup> ( <b>5</b> )	0.00	0.00
CpIr(PH <sub>3</sub> )(C <sub>2</sub> H <sub>5</sub> ) <sup>+</sup> ( <b>6</b> (TS <sub>5–7</sub> ))	0.72	0.38
CpIr(PH <sub>3</sub> )(H)(C <sub>2</sub> H <sub>4</sub> ) <sup>+</sup> ( <b>7</b> )	–12.19	–15.71
C. Ethylene Insertion Reaction		
CpIr(PH <sub>3</sub> )(CH <sub>3</sub> ) <sup>+</sup> , C <sub>2</sub> H <sub>4</sub> ( <b>1</b> + ethylene)	32.04 (29.97) <sup>a</sup>	43.08 (28.68) <sup>a</sup>
CpIr(PH <sub>3</sub> )(CH <sub>3</sub> )(C <sub>2</sub> H <sub>4</sub> ) <sup>+</sup> ( <b>9</b> )	0.00	0.00
CpIr(PH <sub>3</sub> )(CH <sub>3</sub> )(C <sub>2</sub> H <sub>4</sub> ) <sup>+</sup> ( <b>10</b> (TS <sub>9–11</sub> ))	32.84	35.89
CpIr(PH <sub>3</sub> )(C <sub>3</sub> H <sub>7</sub> ) <sup>+</sup> ( <b>11</b> )	9.40	14.75
CpIr(PH <sub>3</sub> )(C <sub>3</sub> H <sub>7</sub> ) <sup>+</sup> ( <b>12</b> (TS <sub>11–13</sub> ))	12.14	19.79
CpIr(PH <sub>3</sub> )(C <sub>3</sub> H <sub>7</sub> ) <sup>+</sup> ( <b>13</b> )	3.61	9.10
D. $\beta$ -H Transfer of CpIr(PH <sub>3</sub> )(C <sub>2</sub> H <sub>3</sub> ) <sup>+</sup>		
CpIr(PH <sub>3</sub> )(C <sub>2</sub> H <sub>3</sub> ) <sup>+</sup> ( <b>14</b> )	0.00	0.00
CpIr(PH <sub>3</sub> )(C <sub>2</sub> H <sub>3</sub> ) <sup>+</sup> ( <b>15</b> (TS <sub>14–16</sub> ))	21.23	17.10
CpIr(PH <sub>3</sub> )(H)(C <sub>2</sub> H <sub>2</sub> ) <sup>+</sup> ( <b>16</b> )	9.41	0.36
E. Acetylene Insertion Reaction		
CpIr(PH <sub>3</sub> )(CH <sub>3</sub> ) <sup>+</sup> , C <sub>2</sub> H <sub>2</sub> ( <b>1</b> + acetylene)	27.97 (25.53) <sup>a</sup>	32.63 (20.05) <sup>a</sup>
CpIr(PH <sub>3</sub> )(CH <sub>3</sub> )(C <sub>2</sub> H <sub>2</sub> ) <sup>+</sup> ( <b>17</b> )	0.00	0.00
CpIr(PH <sub>3</sub> )(CH <sub>3</sub> )(C <sub>2</sub> H <sub>2</sub> ) <sup>+</sup> ( <b>18</b> (TS <sub>17–19</sub> ))	24.83	30.62
CpIr(PH <sub>3</sub> )(C <sub>3</sub> H <sub>3</sub> ) <sup>+</sup> ( <b>19</b> )	–17.50	–3.23

<sup>a</sup> The BSSE correction is included.

plexes.<sup>5</sup> The reaction initially produces a new Ir–alkyl complex through oxidative addition (OA) of alkane, and reductive elimination (RE) of methane then produces an Ir–olefin complex through  $\beta$ -H transfer, as illustrated in Scheme 1. In previous theoretical work,<sup>7</sup> we have shown (i) that the oxidative addition from CpIr(PH<sub>3</sub>)(CH<sub>3</sub>)(agostic-alkane)<sup>+</sup> (**2**) through an OA/RE transition state (TS) (**3**) to CpIr(PH<sub>3</sub>)(CH<sub>3</sub>)(H)(alkyl)<sup>+</sup> (**4**) is endothermic by 4.4 and 0.8 kcal/mol with a low barrier of 11.5 and 10.0 kcal/mol at the DFT-B3LYP and CCSD levels of theory, respectively, (ii) that the reductive elimination from CpIr(PH<sub>3</sub>)(CH<sub>3</sub>)(H)(alkyl)<sup>+</sup> (**4**) through an OA/RE TS (**3**) to a  $\beta$ -agostic complex, CpIr(PH<sub>3</sub>)(alkyl)<sup>+</sup> (**5**), is exothermic with a low barrier of 7.1 and 9.2 kcal/mol, and (iii) that a  $\sigma$ -bond metathesis pathway does not exist for the reaction of free alkanes with the CpIr(PH<sub>3</sub>)(CH<sub>3</sub>)<sup>+</sup> complex (**1**) (see Table 1A). Here, the late stage of alkane dehydrogenation by the CpIr(PH<sub>3</sub>)(CH<sub>3</sub>)<sup>+</sup> complex, the  $\beta$ -hydrogen transfer reaction, will be examined by the B3LYP method.

The B3LYP-optimized geometries for the  $\beta$ -hydrogen transfer reaction of the iridium–ethyl complex from the ethyl complex **5**, through the transition state **6**, to the iridium– $\eta^2$ -ethylene complex **7** are shown in Figure 1. In contrast to the Ir(III)–methyl complex **1**, the Ir(III)–ethyl complex **5** has a very strong  $\beta$ -agostic interaction,<sup>20</sup> where the Ir–H, C $^\alpha$ –C $^\beta$ , and C $^\beta$ –H bonds and Ir–C $^\alpha$ –C $^\beta$  angle are 1.865, 1.514, and 1.220 Å and 79.9°, respectively. In comparison to a “non-agostic” structure, **8**, where the Ir–C $^\alpha$ –C $^\beta$  angle is fixed at 109.5° and all

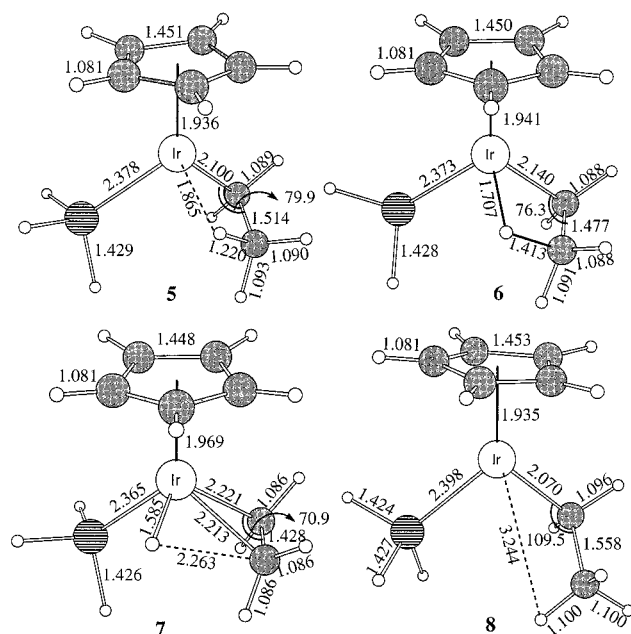


**Figure 1.** B3LYP-optimized geometries for the  $\beta$ -H transfer of the iridium–ethyl complex from the ethyl complex **5** through the transition state **6** to the iridium  $\eta^2$ -ethylene complex **7** and for a non-agostic structure of the ethyl complex **8** (only the average C–C and C–H distances are given for the Cp ring).

other parameters are relaxed during the optimization, these geometrical parameters are very different. The largest change from **5** to **7** appears in the Ir–C (–0.03 Å), C $^\alpha$ –C $^\beta$  (+0.04 Å), and C $^\beta$ –H (–0.12 Å) bonds. From the  $\beta$ -agostic structure **5**, the reaction proceeds toward the  $\beta$ -H transfer through a four-center transition state, **6**, where the Ir–H bond is being formed and the inside C $^\beta$ –H bond is being broken. The small differences between **5** and **6**, Ir–C $^\alpha$ –C $^\beta$  angle (–3.6°), Ir–H bond

(20) (a) Bailey, N. A.; Jenkins, J. M.; Mason, R.; Shaw, B. L. *Chem. Commun.* **1965**, 237. (b) LaPlaca, S. J.; Ibers, J. A. *Inorg. Chem.* **1965**, *4*, 778. (c) Cotton, F. A.; Day, V. W. *J. Chem. Soc., Chem. Commun.* **1974**, 415. (d) Dwoodi, Z.; Green, M. L. H.; Mtetwa, V. S. B.; Prout, K.; Schultz, A. J.; Williams, J. M.; Koetzle, T. F. *J. Chem. Soc., Dalton Trans.* **1986**, 1629. (e) Dwoodi, Z.; Green, M. L. H.; Mtetwa, V. S. B.; Prout, K. *J. Chem. Soc., Chem. Commun.* **1982**, 1410. (f) Brookhart, M.; Green, M. L. H.; Wong, L.-L. *Inorg. Chem.* **1988**, *30*, 1.

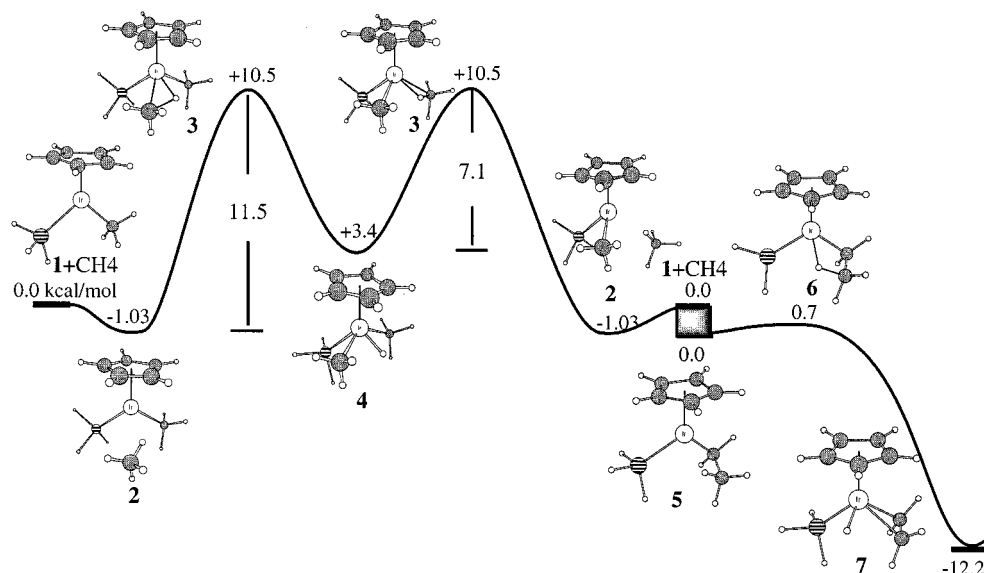


**Figure 2.** B3LYP energy profiles along the OA/RE and  $\beta$ -H transfer pathways from **1** to **7**. In the OA/RE reaction stage, the energy numbers are relative to the total energy of reactants **1** and  $\text{CH}_4$ . In the  $\beta$ -H transfer reaction stage, the energy numbers are relative to the Ir alkyl complex **5**.

( $-0.158 \text{ \AA}$ ),  $\text{C}^\alpha\text{--C}^\beta$  bond ( $-0.037 \text{ \AA}$ ), and inside  $\text{C}^\beta\text{--H}$  bond ( $+0.193 \text{ \AA}$ ), point to a very early transition state. In the  $\beta$ -H transfer product **7**, an olefin hydride complex, the metal center is very close to the olefin, where the Ir–C distances are only longer by about  $0.16 \text{ \AA}$  (experimental  $0.07 \text{ \AA}$ ) than that of **1**. However, the C=C bond distance of **7**,  $1.428 \text{ \AA}$ , is clearly longer by  $0.08 \text{ \AA}$  (experimental  $0.09 \text{ \AA}$ ) than that of a free ethylene.<sup>5</sup> In addition, the Cp–Ir centroid distance of **7** is longer by about  $0.03 \text{ \AA}$  and the Cp ring has slipped more than that of **5** and **6**. Such a structural feature in the  $\pi$ -complex **7** is similar to that in the OA/RE intermediate **4**.<sup>7c,21</sup> Thus, because of a strong back-donating interaction between ethylene and the metal center, the Ir–ethylene bond becomes more covalent, reducing the C–C bond order and making the Ir center formally Ir(V).

The B3LYP and CCSD//B3LYP relative energies of  $\beta$ -H transfer from the iridium–ethyl complex **5**, through the transition state **6**, to the  $\pi$ -complex **7** are shown in Figure 2 (Figure 2 also shows the early OA/RE stages<sup>7c</sup>) and Table 1B. The overall reaction is exothermic by  $12.2$  and  $15.7$  kcal/mol with a very low activation barrier of  $0.7$  and  $0.4$  kcal/mol at the B3LYP and CCSD//B3LYP levels, respectively. The larger exothermicity calculated at the CCSD//B3LYP level arises because B3LYP underestimates the metal–ligand bond energy. In comparison to the “non-agostic” structure **8**, the iridium–ethyl complex **5** is more stable by  $5.0$  and  $7.7$  kcal/mol. Clearly, the  $\beta$ -agostic interaction of **5** is stronger by  $0.3$  and  $1.4$  kcal/mol than the agostic interaction of **2**. This reaction is substantially different from that of early-transition-metal complexes, where the  $\beta$ -H transfer, a chain termination step, is endothermic with a high activation barrier. Because the  $\beta$ -H transfer reaction of the Ir(III)–alkyl complexes takes place more easily than the OA/RE reaction, the rate-determining step of

the activation of alkanes to olefin complexes by  $\text{Cp}^*\text{Ir}(\text{PMe}_3)(\text{CH}_3)^+$  is the alkane OA/RE step.

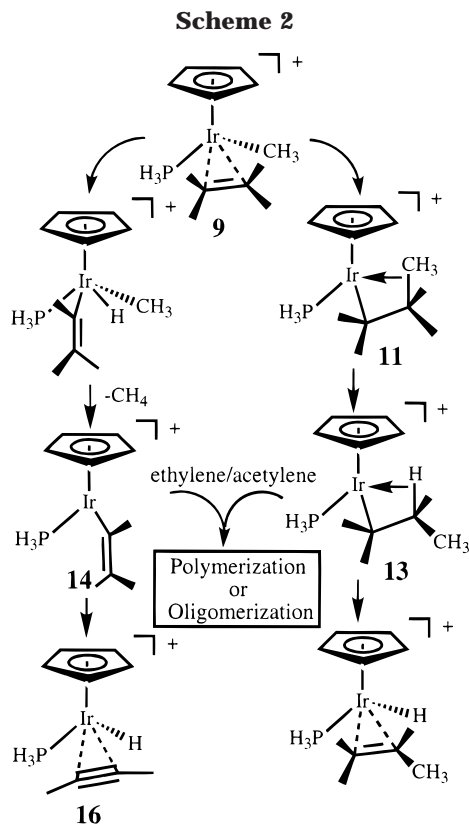
A more recent study reported an iridium catalytic system,  $\{\eta^3\text{-C}_6\text{H}_3[\text{CH}_2\text{P}(\text{tert-C}_4\text{H}_9)_2]_2\}\text{Ir}(\text{H})_2$ ,<sup>6</sup> which converts alkanes to alkenes without a hydrogen acceptor. The mechanism for this catalytic system should be similar to that of the cationic iridium complex  $\text{Cp}^*\text{Ir}(\text{PR}_3)(\text{CH}_3)^+$ . However, the steric and electronic effects of the spectator ligands can play key roles in alkane dehydrogenations catalyzed by transition-metal complexes.<sup>22</sup>

**Ethylene Insertion into the Ir– $\text{CH}_3$   $\sigma$ -Bond.** The possible reactions of the iridium–alkene complex are substantially different from those of the iridium–alkane complex, since the alkane can yield an iridium–alkenyl complex through an OA/RE process or an iridium–alkyl complex through an insertion process. A  $\beta$ -H transfer can occur following either of these initial processes. Thus, reactions of ethylene with the  $\text{CpIr}(\text{PH}_3)(\text{CH}_3)^+$  complex may result in new complexes and products, as illustrated in Scheme 2. In previous work, we have mentioned that the high barriers of  $34$  kcal/mol and endothermicities of  $22\text{--}31$  kcal/mol make the oxidative addition reaction for ethylene much more difficult than that for methane.<sup>7c</sup> In this section, we will examine the possibility of an ethylene insertion reaction.

The B3LYP fully optimized geometries of the  $\pi$ -complex **9**, the insertion TS **10**,  $\gamma$ -agostic intermediate **11**, rotation TS **12**, and  $\beta$ -agostic product **13** are shown in Figure 3. The Ir–ethylene  $\pi$ -complex **9** displays structural features very similar to those of complex **7** in the longer Ir–Cp and Ir– $\text{CH}_3$  bonds, which are characteristic of an Ir(V) complex as mentioned above. The substantial difference between the  $\pi$ -complex **9** and that of an early transition metal arises because of a particularly strong back-donation from Ir to ethylene. In comparison to a free ethylene molecule, the C–C double bond of **9** is longer by  $0.080 \text{ \AA}$ , and the distances

(21) The optimized geometry of  $\text{CpIr}(\text{PH}_3)(\text{CH}_3)^{3+}$  shows a structural feature similar to that of  $\text{CpIr}(\text{PH}_3)(\text{H})(\text{CH}_3)(\text{R})^+$  ( $\text{R} = \text{CH}_3, \text{C}_2\text{H}_5, \text{C}_2\text{H}_5$ ) with a slipped Cp ring and coordinating fashion. Niu, S.-Q.; Hall, M. B. Unpublished work.

(22) Niu, S.-Q.; Hall, M. B. *J. Am. Chem. Soc.*, submitted for publication.



between Ir and the carbon of the ethylene are close to that of a normal Ir–C bond. The main feature in the first step of this reaction,  $\pi$ -complex **9** to insertion transition state **10**, is migration of the methyl ligand. After the ethylene inserts into the Ir–CH<sub>3</sub>  $\sigma$ -bond, an iridium–propyl complex, **11**, is formed. The inside C $\gamma$ –H bond is longer by about 0.05 Å than the normal C–H single bond. This structural feature points to the presence of an Ir–H–C  $\gamma$ -agostic interaction in **11**. As the methyl rotates, a new transition state (**12**) is followed by a new isomer (**13**), in which the inside C $\beta$ –H is longer by 0.16 Å than a normal C–H bond and the Ir–C $\alpha$ –C $\beta$  angle is smaller by 29.2° than a standard sp<sup>3</sup> hybrid angle (109.5°). In comparison to the ethyl  $\beta$ -agostic complex **5**, the propyl complex **13** has a shorter Ir–H (–0.062 Å) and a longer C $\beta$ –H bond (+0.044 Å). Clearly, the  $\beta$ -position substituent effect has a strong influence on the  $\beta$ -agostic interaction.

The relative energies calculated at the B3LYP and CCSD//B3LYP levels for this insertion process are summarized in Figure 4 and Table 1C. The calculated ethylene association energy before any BSSE correction is –32.04 and –43.08 kcal/mol at the B3LYP and CCSD//B3LYP levels, respectively, and –29.97 and –28.68 kcal/mol after the BSSE correction. Clearly, the BSSE correction is much larger for the CCSD binding energy. As we have discussed above, this system differs from early-transition-metal complexes in having a stronger back-bonding interaction between olefin and metal as in the complex **9**. The larger ethylene association energy leads to a high barrier for the loss of olefin and prevents the formation of a dehydrogenation catalytic cycle. The calculated results are consistent with the fact that only **7** has only been observed experimentally, and a catalytic cycle has not been seen.<sup>5,7e</sup>

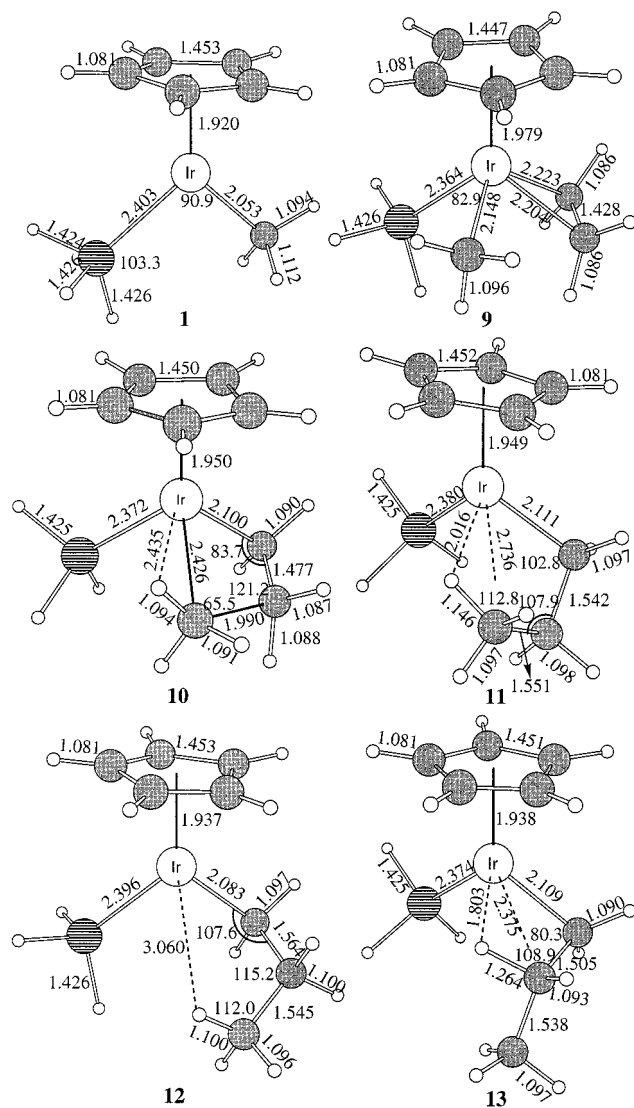


**Figure 3.** B3LYP fully optimized geometries of the reactant (**1**),  $\pi$ -intermediate (**9**), insertion TS (**10**),  $\gamma$ -agostic intermediate (**11**), rotation TS (**12**), and  $\beta$ -agostic product (**13**) along the insertion pathway (only the average C–C and C–H distances are given for the Cp ring).

For ethylene, **9** is more stable by 4 and 9 kcal/mol at the B3LYP and CCSD//B3LYP levels, respectively, than the  $\beta$ -agostic structure **13**. Ethylene insertion from the  $\pi$ -complex **9** through transition state **10** to form the  $\gamma$ -agostic complex **11** is endothermic by 9 and 15 kcal/mol with a high activation barrier of 33 and 36 kcal/mol at the B3LYP and CCSD//B3LYP levels, respectively.<sup>23</sup> The  $\beta$ -agostic complex **13** is more stable by 4–6 kcal/mol than the  $\gamma$ -agostic complex **11**; the rotation barrier from **11** to **13** is 3–5 kcal/mol. The relative energy differences between B3LYP and CCSD//B3LYP arise from underestimated metal–ligand binding energies at the B3LYP level. Here, the CCSD//B3LYP values for the ethylene insertion reaction are more endothermic (Table 1C), since the ethylene insertion

(23) (a) Han, Y.-Z.; Deng, L.-Q.; Ziegler, T. *J. Am. Chem. Soc.* **1997**, *119*, 5939. (b) In ref 23a, Han et al. showed that this reaction is slightly endothermic by 1.2 kcal/mol with a barrier of 23.2 kcal/mol by BP86//LDA calculations. In comparison to the X-ray and B3LYP-optimized geometry of the Ir–olefin  $\pi$ -complex, the back-donating interaction between the metal center and olefin is underestimated at the LDA level.

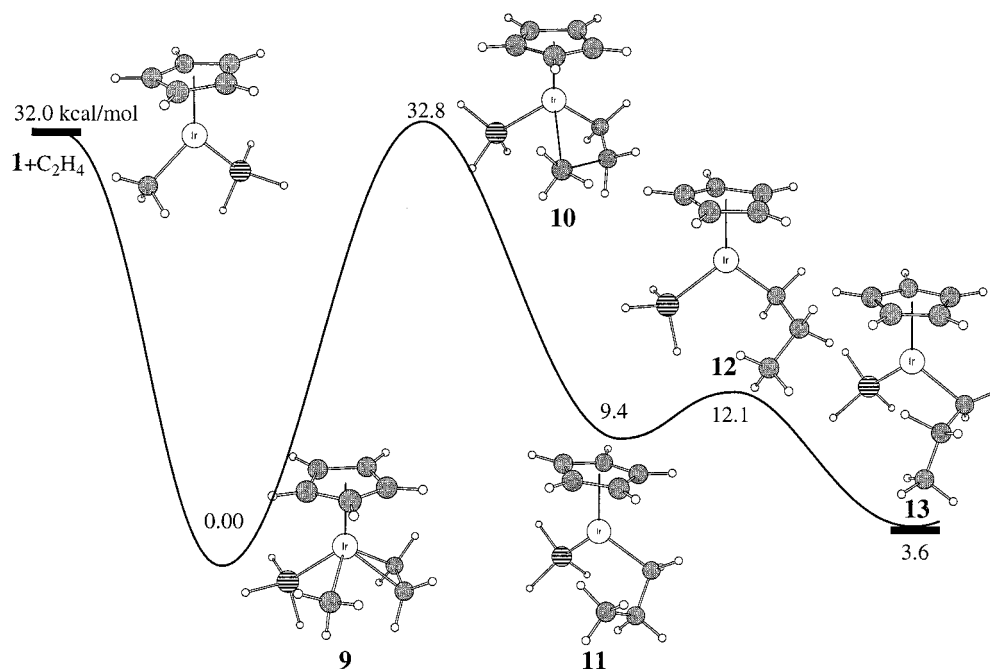


**Figure 4.** B3LYP energy profiles along the ethylene insertion pathway from **1** to **13**.

reaction bears some similarity to the reverse of the  $\beta$ -H transfer of the iridium ethyl complex (Table 1B). Overall, the reaction from the reactants (**1** and ethylene) to  $\beta$ -agostic complex **13** is exothermic with a high barrier. Thus, like the ethylene C–H bond OA/RE process,<sup>7c</sup> the ethylene insertion reaction would not take place at low temperature.

**$\beta$ -H Transfer in the Ir(III) Vinyl Complex.** The iridium vinyl complex formed by ethylene OA/RE could undergo  $\beta$ -H transfer to form an iridium–acetylene complex as shown in Scheme 2. The B3LYP-optimized geometries for this process from the iridium–vinyl complex **14** through the transition state **15** to the iridium  $\eta^2$ -acetylene complex **16** are shown in Figure 5.

In the Ir–vinyl complex **14**, the Ir–C $^{\alpha}$ –C $^{\beta}$  and C $^{\alpha}$ –C $^{\beta}$ –H angles are larger by about 3–4° than the standard sp<sup>2</sup> hybrid angle (120°). This “non-agostic” structural feature is very different from that of early-transition-metal–propenyl complexes, where the M–C $^{\alpha}$ –C $^{\beta}$  angle is smaller by about 20° than the standard sp<sup>2</sup> hybrid angle (120°).<sup>24</sup> The shorter Ir–C $^{\alpha}$  and longer C $^{\alpha}$ –C $^{\beta}$  bonds in the Ir–vinyl complex **14** are indicative of a strong  $\pi$ -donating interaction between the metal center and vinyl ligand of **14**, as illustrated in Chart 1. Thus, Ir–vinyl complex **14** favors a strong  $\pi$ -donating interaction clearly leads to a longer C $^{\alpha}$ –C $^{\beta}$  bond in the Ir–vinyl complex.

As the vinyl ligand rotates and bends, a  $\beta$ -agostic interaction structure, **15**, is formed at the saddle point, where the Ir–C $^{\alpha}$ –C $^{\beta}$  angle is smaller by 37°, the inside C $^{\beta}$ –H and Ir–C $^{\alpha}$  bonds are longer by 0.088 and 0.084 Å, respectively, and the C $^{\alpha}$ –C $^{\beta}$  bond is shorter by 0.039 Å with respect to **16**. From the transition state **15** to the acetylene  $\pi$ -complex **16**, the inside C $^{\beta}$ –H bond is

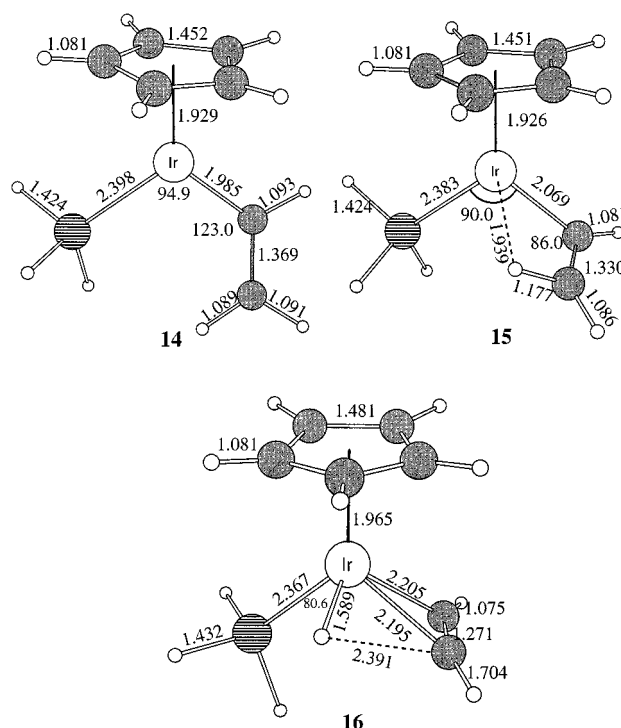


**Figure 5.** B3LYP-optimized geometries for the  $\beta$ -hydrogen transfer of the iridium–vinyl complex from the vinyl complex **14** through the transition state **15** to the iridium  $\eta^2$ -acetylene complex **16** (only the average C–C and C–H distances are given for the Cp ring).

broken and the Ir–H bond is formed. Like the ethylene  $\pi$ -complexes (**7** and **9**), **16** has a Cp(centroid)–Ir distance which is longer by about 0.04 Å than that of the transition state **15** or the vinyl complex **14**. The strong  $\pi$ -back-donation interaction between acetylene and the metal center, as in the case of ethylene, leads to a slipped Cp–Ir interaction.

The relative energies of this  $\beta$ -H transfer from iridium vinyl complex **14** to the iridium  $\eta^2$ -acetylene complex **16** are shown in Figure 6 and Table 1D. The reaction

(24) (a) Yoshida, T.; Koga, N.; Morokuma, K. *Organometallics* **1995**, *14*, 746. (b) Hyla-Kryspin, I.; Niu, S.; Gleiter, R. *Organometallics* **1995**, *14*, 964.

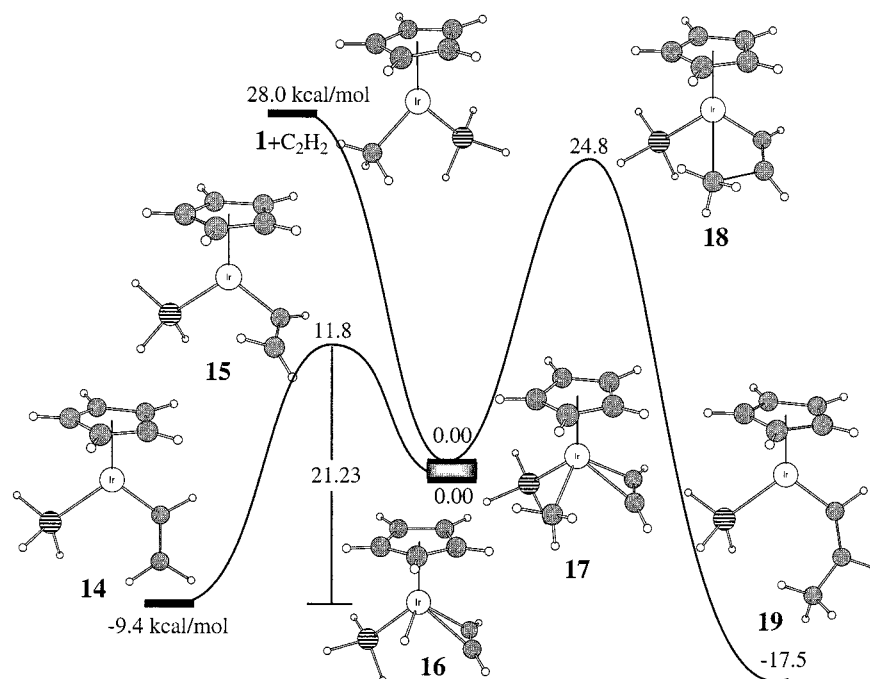
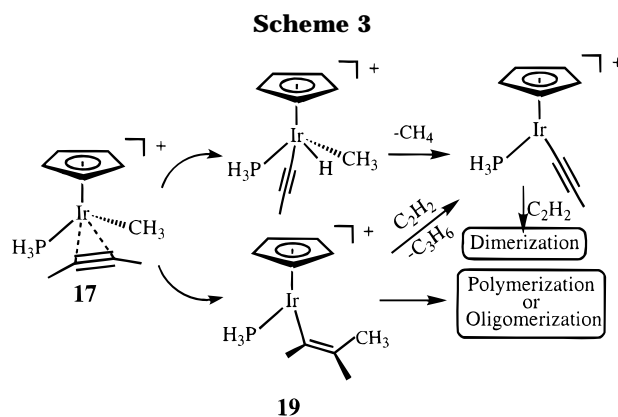
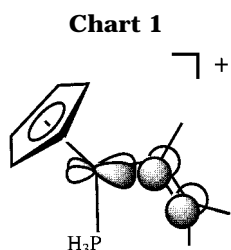


**Figure 6.** B3LYP energy profiles along the  $\beta$ -hydrogen transfer pathway from the vinyl complex **14** through the transition state **15** to the iridium  $\eta^2$ -acetylene complex **16**, where the energy numbers are relative to the Ir-alkyl complex **16**, and along the insertion pathway from reactants **1** and acetylene through **17** and **18** to **19**, where the energy numbers are relative to the Ir-alkyl complex **17**.



is endothermic by 9.4 and 0.4 kcal/mol with an activation barrier of 21.2 and 17.1 kcal/mol at the B3LYP and CCSD//B3LYP levels, respectively. Again, in comparison to the CCSD//B3LYP calculation, the B3LYP calculations, by underestimating the Ir-acetylene binding energy, result in a larger endothermicity for the  $\beta$ -H transfer of  $\text{CpIr}(\text{PH}_3)(\text{C}_2\text{H}_3)^+$  (see Table 1D). Although the  $\beta$ -agostic interaction does not stabilize an equilibrium structure for the Ir(III) vinyl complex, it leads to a low activation barrier for this reaction. Thus, the reverse reaction of the  $\beta$ -H transfer, acetylene insertion into an Ir-H  $\sigma$ -bond, is kinetically and thermodynamically favorable.

**Acetylene Insertion into the Ir-CH<sub>3</sub>  $\sigma$ -Bond.** Recent experimental work shows that OA/RE and insertion reactions play important roles in the dimerization of terminal alkynes by late-transition-metal catalysts.<sup>10</sup> The cationic iridium-acetylene complex is similar to the iridium-ethylene complex in chemical behavior. As shown in Scheme 3, the acetylene  $\pi$ -complex **17** can undergo either oxidative addition to give an iridium-acetylide complex or insert into an Ir-alkyl bond to give an iridium-vinyl complex. Thus, reactions of acetylene with  $\text{CpIr}(\text{PH}_3)(\text{CH}_3)^+$  complex (**1**) may result in several new products. In previous work, we have shown that the OA/RE reaction of acetylene with the iridium complex, although not facile, does take place

more easily than that of the ethylene, where the reaction from the  $\pi$ -complex **17** to the acetylide complex is endothermic by 5–14 kcal/mol with a barrier of 24–32 kcal/mol.<sup>7c</sup> Here, the possible acetylene insertion reaction will be investigated.

The acetylene insertion proceeds from the  $\pi$ -complex (**17**) through the transition state (**18**) to the vinyl complex (**19**). The B3LYP-optimized geometries of the  $\pi$ -complex **17**, TS **18**, and vinyl complex **19** are shown in Figure 7. The acetylene  $\pi$ -complex **17** is similar to the ethylene  $\pi$ -complex **9**; both show longer Cp-Ir and Ir-CH<sub>3</sub> distances than those of the iridium-alkane complex. The C-C triple bond is longer by 0.049 Å than the C-C triple bond in the free acetylene molecule. Again, these structural features show that there is a strong back-donating interaction between acetylene and the metal center. However, this interaction should be weaker than that of the iridium-ethylene  $\pi$ -complex, as illustrated by the smaller change in C-C and Cp-Ir distances (vide infra). As the methyl ligand migrates to the acetylene to form TS **18**, Ir-C $^{\gamma}$  and C $^{\beta}$ -C $^{\gamma}$  distances are longer by 0.241 and shorter by 0.753 Å,

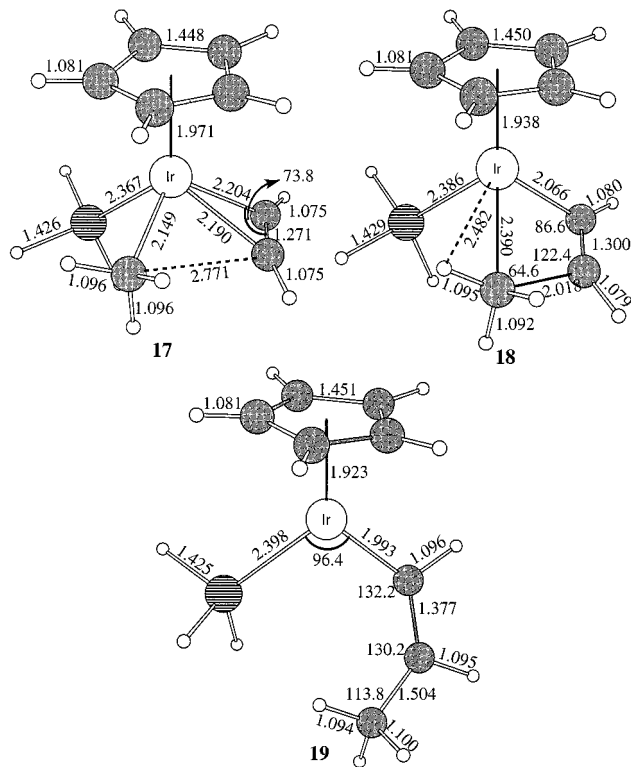


**Figure 7.** B3LYP-optimized geometries of the  $\pi$ -intermediate **17**, transition state **18**, and vinyl complex **19** along the insertion pathway (only the average C–C and C–H distances are given for the Cp ring).

respectively, than those in the corresponding  $\pi$ -complex **17**. Thus, the acetylene insertion effectively has a later TS. In the product Ir–vinyl complex **19**, the Ir–C $^{\alpha}$ –C $^{\beta}$  and C $^{\alpha}$ –C $^{\beta}$ –C $^{\gamma}$  angles are larger by about 10° than the standard sp<sup>2</sup> hybrid angle (120°). “Non-agostic” structures, like **19** and **14**, show a characteristic feature of an electron-deficient late-transition-metal–vinyl complex, where strong  $\pi$ -bonding (as shown in Chart 1) is favored over the agostic bonding, a feature which is very different from that found in early-transition-metal vinyl complexes.<sup>24</sup>

As seen from Figure 6 and Table 1E, the calculated acetylene association energy before the BSSE correction is –27.97 and –32.63 kcal/mol at the B3LYP and CCSD//B3LYP levels, respectively, and –25.53 and –20.05 kcal/mol after the BSSE correction. Clearly, the B3LYP BSSE correction overestimates the metal–acetylene binding energy with respect to the CCSD//B3LYP BSSE correction. Since the B3LYP calculation underestimates the Ir–ligand binding energy with respect to the CCSD//B3LYP calculation, the energy profiles for the acetylene insertion process show that the reaction from the  $\pi$ -complex **17** and acetylene to **19** is more exothermic by 14.27 kcal/mol at the B3LYP than that at the CCSD//B3LYP level. Nevertheless, the acetylene insertion step from the  $\pi$ -complex **17** through transition state **18** to vinyl complex **19** is exothermic by 18 and 3 kcal/mol with an activation barrier of 25 and 31 kcal/mol. Thus, although neither acetylene insertion nor oxidative addition of acetylene to the iridium complex is a low-temperature process, both reactions do take place more easily than those of the ethylene. Reactions of acetylene with the CpIr(PH<sub>3</sub>)–

(CH<sub>3</sub>)<sup>+</sup> complex could result in dimerization products, especially for sterically hindered terminal alkynes.<sup>10</sup>

## Conclusions

The alkane dehydrogenation catalyzed by CpIr(PH<sub>3</sub>)–(CH<sub>3</sub>)<sup>+</sup> (**1**) generates CpIr(PH<sub>3</sub>)(H)(olefin)<sup>+</sup> in three low-energy steps: (i) oxidative addition from CpIr(PH<sub>3</sub>)–(CH<sub>3</sub>)(alkane)<sup>+</sup> to CpIr(PH<sub>3</sub>)(CH<sub>3</sub>)(H)(alkyl)<sup>+</sup> is endothermic by about 0.8–4.4 kcal/mol with a low barrier of 10.0–11.5 kcal/mol, (ii) reductive elimination from CpIr(PH<sub>3</sub>)(CH<sub>3</sub>)(H)(alkyl)<sup>+</sup> to a  $\beta$ -agostic structure iridium–alkyl complex, CpIr(PH<sub>3</sub>)(alkyl)<sup>+</sup> + CH<sub>4</sub>, is exothermic with a low barrier of 7.1–9.2 kcal/mol, and (iii)  $\beta$ -H transfer from CpIr(PH<sub>3</sub>)(alkyl)<sup>+</sup> to CpIr(PH<sub>3</sub>)(H)(olefin)<sup>+</sup> is exothermic by 12–16 kcal/mol with a very low barrier of 0.4–0.7 kcal/mol. The rate-determining step for the activation of alkanes by Cp\*Ir(PMe<sub>3</sub>)(CH<sub>3</sub>)<sup>+</sup> and their conversion to olefin complexes is the alkane oxidative-addition step. Kinetically, the strong  $\beta$ -agostic interaction of iridium–alkyl complexes leads to a stabilization of the CpIr(PH<sub>3</sub>)(alkyl)<sup>+</sup> complex and lower activation energy for the  $\beta$ -H transfer. Thermodynamically, the strong stabilizing interaction of ethylene with CpIr(PH<sub>3</sub>)(CH<sub>3</sub>)<sup>+</sup> leads to a chemical equilibrium lying toward the iridium–olefin product.

Because of a strong association of ethylene and acetylene with CpIr(PH<sub>3</sub>)(CH<sub>3</sub>)<sup>+</sup> (**1**), their insertion reactions are high-energy processes, with barriers of 24–36 kcal/mol. In comparison to ethylene, the insertion reaction of acetylene with the CpIr(PH<sub>3</sub>)(CH<sub>3</sub>)<sup>+</sup> complex is more favorable. More sterically hindered Ir ethylene or acetylene complexes would favor the insertion reaction by decreasing the stability of the  $\pi$ -complexes.

The third-row transition-metal complexes undergo oxidative-addition reactions, M<sup>I</sup> + A–B → M<sup>III</sup>(A)(B), more easily than their second-row transition-metal congeners because late third-row transition metals have either d<sup>9</sup>s<sup>1</sup> ground states or d<sup>8</sup>s<sup>1</sup> low-lying excited states, while late second-row transition metals have d<sup>n+1</sup> ground states with high-lying d<sup>n</sup>s<sup>1</sup> excited states.<sup>15,25</sup> This view emphasizes the importance of forming sd hybrids for the two new covalent bonds in the product. The origin of the atomic differences has been attributed to relativistic effects,<sup>26</sup> which stabilize the (n + 1)s orbitals and destabilize the nd orbitals more for the heavier third-row transition metals. On the other hand, since the redox ability of transition metals is reflected by their ionization potential (IP), the energy gap between the metal and ligand is directly proportional to the IP of the transition metal. Thus, the oxidative-addition reaction M<sup>III</sup> + A–B → M<sup>V</sup>(A)(B) for M = Ir proceeds more easily than that for M = Rh because Ir(III) has a smaller ionization energy than Rh(III).<sup>7b,27</sup>

(25) (a) Low, J. J.; Goddard, W. A., III. *J. Am. Chem. Soc.* **1986**, *108*, 6115. (b) Low, J. J.; Goddard, W. A., III. *J. Am. Chem. Soc.* **1984**, *106*, 8321. (c) Low, J. J.; Goddard, W. A., III. *J. Am. Chem. Soc.* **1984**, *106*, 6928.

(26) (a) Pyykkö, P. *Chem. Rev.* **1988**, *88*, 563. (b) Schwarz, W. H. E.; van Wezenbeek, E. M.; Baerends, E. J.; Snijders, J. G. *J. Phys. B* **1989**, *B22*, 1515. (c) Wezenbeek, E. M.; Baerends, E. J.; Ziegler, T. *Inorg. Chem.* **1995**, *34*, 238. (d) The Hay-Wadt ECPs include relativistic effects.

(27) (a) Shriver, D. F.; Atkins, P. W.; Langford, C. H. *Inorganic Chemistry*; W. H. Freeman: New York, 1990. (b) The transition-metal IP values for high valence states can be obtained from the experimental IP values for lower valence states by extrapolation.



Because of a strong  $\pi$ -accepting interaction of ethylene and acetylene with late transition metals, these ligands can effectively pull electrons away from the metal and act as if they were partially oxidizing the metal. As the covalent bond between the metal and these ligands becomes strong, the ligands become formally  $C_2H_4^{2-}$  and  $C_2H_2^{2-}$  and the electronic structure of the late-transition-metal  $\pi$ -complex approaches a formal  $M^{N+2}$  state, much as it does in the OA reaction above. Thus, the insertion reaction can be considered as a reduction process:  $M^{N+2} \rightarrow M^N$ . On the basis of this view, the ethylene and acetylene insertions into the M-R  $\sigma$ -bond for M = Rh proceed more easily than those for M = Ir.<sup>23a</sup> By following the ionization potential of late transition metals, one can predict that, in contrast

to the oxidative-addition reactions, the ease of ethylene or acetylene insertion is Os(II) < Ru(II)  $\leq$  Pt(II) < Pd(II).

**Acknowledgment.** We thank the Robert A. Welch Foundation (Grant A-648) and the National Science Foundation (CHE 94-23271, 95-28196, and 98-00184), for financial support. This research was conducted in part with use of the Cornell Theory Center, a resource for the Center for Theory and Simulation in Science and Engineering at Cornell University, which is funded in part by the National Science Foundation, New York State, and IBM Corp.

OM980429N